

## X-ray Powder Diffraction Study on the MgB<sub>2</sub> Superconductor with nano-SiC additions: The Effects of Sintering Temperature

Tan Kwee Yong<sup>1,\*</sup>, Tan Kim Lee<sup>1</sup>, Abdul Halim Shaari<sup>1</sup>, Tan Kar Ban<sup>2</sup>, and Chen Soo Kien<sup>1</sup>

**Abstract** — SiC added MgB<sub>2</sub> polycrystalline samples were synthesized at low (650°C) and high (850°C) temperatures in order to study the sintering effect on the phase formation and superconducting properties. The MgB<sub>2</sub> bulks with addition of 0wt%, 1wt%, 3wt% and 5wt% were studied with powder X-ray diffraction technique. We observed that MgB<sub>2</sub> remained as the primary phase for both sintering temperature in all samples with the presence of MgO and Mg<sub>2</sub>Si as the main impurities. Some diffraction peaks associated with unreacted SiC is also noticeable. The intensity of the Mg<sub>2</sub>Si peaks was found to decrease in samples sintered at higher temperature. Temperature dependent magnetic moment measurement showed that the superconducting transition temperature, T<sub>c</sub> decreases as the SiC addition level increases while lower sintering temperature degrade T<sub>c</sub> to greater extent. The changes in the physical properties is discussed based on the results of phase formation, full width half maximum (FWHM), lattice parameter and crystallite size.

**Keywords:** MgB<sub>2</sub>, sintering temperature, SiC, XRD.

### I. INTRODUCTION

SINCE the discovery of MgB<sub>2</sub> by J. Akimitsu in 2001 [1], much research has been done owing to its fascinating properties of high transition temperature (T<sub>c</sub>), large coherence length, small anisotropy and other unique features [2] showing potentiality for commercialization replacing the conventional Nb-based superconductors.

Tan Kwee Yong\*, Tan Kim Lee, Abdul Halim Shaari and Chen Soo Kien are with the Dept. of Physics, Faculty of Science, Universiti Putra Malaysia, 43400 UPM Serdang, Malaysia (\*corresponding author's phone: +6016-7688345; fax: +603-8946 4454; e-mail: kweeyong@gmail.com).

Tan Kim Lee (e-mail: faviscamp@hotmail.com).

Abdul Halim Shaari (e-mail: ahalim@science.upm.edu.my).

Chen Soo Kien (e-mail: skchen@science.upm.edu.my).

Tan Kar Ban is with the Dept. of Chemistry, Faculty of Science, Universiti Putra Malaysia, 43400 UPM Serdang, Malaysia (e-mail: tankb@science.upm.edu.my).

Various studies have been concentrated on the synthesis of high purity MgB<sub>2</sub> by using various methods [3-5] and fabrication of wires [6], tapes [7] or thin films [8]. Much work has also been carried out in improving its critical current density (J<sub>c</sub>) by creating defects or introducing impurities by doping with metals [9], inorganic elements [10], organic compounds [11] and rare earth elements [12,13]. Dou *et al* showed that nano-SiC is able to enhance the J<sub>c</sub> of MgB<sub>2</sub> to as high as ~10<sup>4</sup> A/cm<sup>2</sup> at 6T and 5K [14]. There has been widely known that SiC reacts with Mg to form Mg<sub>2</sub>Si, releasing carbon to dope into the MgB<sub>2</sub> structure, replacing the boron atom. Thus, it is believed that the carbon with one extra electron than boron will donate this electron to the σ band [15-18]. In particular, studies have been converged mainly at carbon based doped MgB<sub>2</sub> that is able to enhance the J<sub>c</sub> by creating lattice defects [19,20]. Reports have shown that C-doping is favourable at higher temperature than at lower temperature. Mudgel *et al* have shown that Mg-B-C compound started to form at 850°C for 2 hours sintering [21]. In this study, we report the effect of sintering temperature on nano-SiC added MgB<sub>2</sub> sintered at low (650°C) and high (850°C) temperature with its phase and crystalline properties that were investigated through X-ray powder diffraction and its T<sub>c</sub> measurement.

### II. METHODOLOGY

Magnesium (Tangshan, 99%), amorphous Boron (Pfaltz & Bauer, 99%) and nano-Silicone Carbide (Nano-Amor, 15nm, 99+%) were used to prepare the samples via *in-situ* solid state reaction method. These powders were weighed according to the stoichiometric ratio of Mg:B:SiC = 1:2:x where x = 0wt%, 1wt%, 3wt%, 5wt% relative to the weight of the MgB<sub>2</sub> samples prepared. The mixture was then pressed into 13mm diameter pellets after a thorough mixing for 2 hours. The pellets were sealed inside SUS306 stainless steel tubes in order to minimize the contact with sintering atmosphere. Argon gas was subsequently flown through the furnace during the whole sintering process. The pellets were sintered at 650°C and 850°C respectively for 1 hour with the heating and cooling rates of 10°C/min. Sintered samples were then crushed and ground into powder for diffraction using X'Pert Pro Panalytical PW3040 MPD X-ray Diffractometer with Cu anode. The crystalline properties of the samples were analyzed by the Rietveld Refinement

using the PanAnalytical X'pert Highscore and X'pert Plus.  $T_c$  measurements were carried out by using a Quantum Design-Magnetic Property Measurement System (MPMS).

### III. RESULTS AND DISCUSSIONS

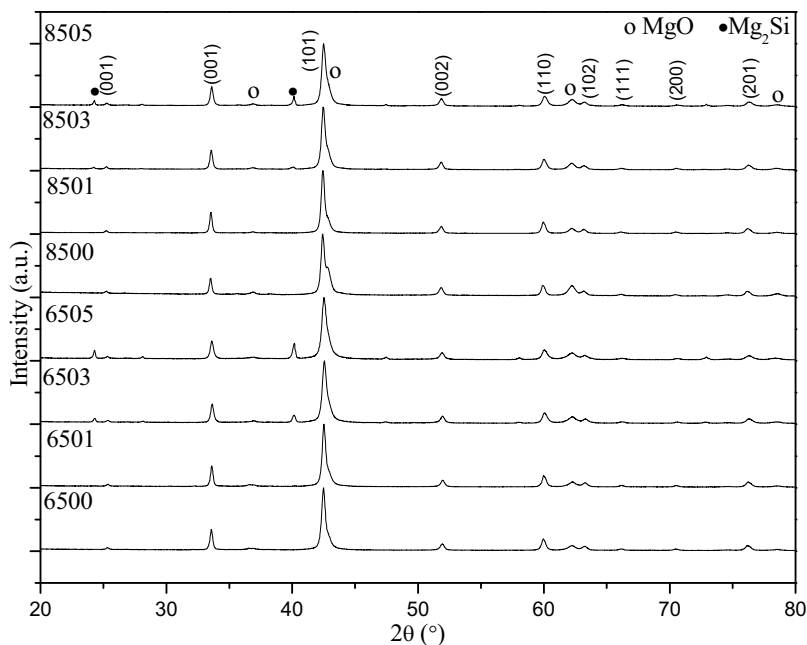


Figure 1: XRD spectra of the various sintered samples.

Table 1: Sintering temperature and addition level with sample identity

Sintering Temperature (°C)	Addition Level (wt%)	Sample Identity
650	0	6500
	1	6501
	3	6503
	5	6505
850	0	8500
	1	8501
	3	8503
	5	8505

Each sample with the respective addition level and sintering temperature is denoted with an identity for the ease of discussion as shown in table 1. Figure 1 showed the XRD spectra of the various samples sintered at both high and low temperatures. All  $MgB_2$  peaks are identified and indexed at the top layer of the spectra. Pure samples were prepared as reference for both temperatures. It is found that all the samples showed  $MgB_2$  as the primary phase with detectable amount of MgO. Oxidation of Mg is inevitable as Oxygen is one of the atmospheric gases and it was entrapped inside the tubes well before sintering. For low temperature sintered samples, it was found that there is no unreacted Mg in samples 6500-6505 indicating all the Mg have been used up to form primary and secondary phases. As the addition of SiC increases,  $Mg_2Si$  peaks started to be revealed in 6503 and its peak became more significant in 6505.  $Mg_2Si$  is a very common secondary phase in SiC doped  $MgB_2$  as the

reaction between Mg and SiC started as low as 500°C [22] well before the reaction between Mg-B takes place. For high temperature sintering, there is no unreacted Mg detected in 8500-8505. It is also found that these samples do not show higher boride phases such as  $MgB_4$  or  $MgB_7$  which are expected to exist at high temperature sintering due to Mg vaporization. With increasing addition level, high temperature sintered samples only show relatively significant  $Mg_2Si$  peak in 8505. By comparing all samples, low temperature sintering is able to produce more secondary phases than high temperature as 6503 and 6505 gave relatively higher  $Mg_2Si$  peak intensity with respect to 8503 and 8505. Qu *et al* reported that  $Mg_2Si$  has higher Gibbs' Free Energy at lower temperature [22], which is in agreement with our studies. Although lower temperature favors the reaction between SiC and Mg, there is no higher boride phase to be formed also, probably means that low temperature sintering is able to retain more Mg. Moreover, there is no unreacted SiC found in the SiC added samples indicating that all SiC have undergone reaction.

Table 2: Phase analysis of various samples

Sample	Relative Intensity Fraction of Phase X (%)		Density (g/cm <sup>3</sup> )	Density ratio
	MgO	Mg <sub>2</sub> Si		
6500	4.67	0.00	1.4183	0.5562
6501	3.64	0.00	1.3942	0.5468

<b>6503</b>	5.20	6.49	1.4871	0.5832
<b>6505</b>	5.58	12.07	1.4052	0.5511
<b>8500</b>	8.50	0.00	1.4099	0.5529
<b>8501</b>	4.08	0.00	1.4073	0.5519
<b>8503</b>	5.29	1.79	1.4269	0.5596
<b>8505</b>	5.72	8.10	1.4112	0.5534

Table 2 showed the phase analysis of the samples sintered at both temperatures.

The relative intensity fractions of phase were generated according to [23]. Among the samples, 6501 showed the lowest percentage for both MgO and Mg<sub>2</sub>Si with 3.64% and 0.00% respectively, while 6505 gives the highest Mg<sub>2</sub>Si fraction at 12.07% and 8500 produces highest MgO of 8.50%. With increasing SiC addition, the relative intensity fraction of Mg<sub>2</sub>Si increases indicating that more SiC has undergone reaction with Mg. As the temperature increases, percentage of MgO varies slightly overall for SiC added samples compared to low temperature sintered samples. The relative intensity fractions calculated is in accordance with [22] as low temperature sintering will give higher fraction of Mg<sub>2</sub>Si compare to high temperature as can be seen in 6505 and 8505. Both sintering temperatures, however, do not affect the density of the samples. The density of the samples range from 1.39 to 1.48g/cm<sup>3</sup> giving the density ratio ( geometrical density to the theoretical density of MgB<sub>2</sub> [14] ) of 0.54-0.58 which is much lower than can be achieved for hot pressed 5wt% SiC added samples at 850°C (1.7g/cm<sup>3</sup>) [22].

Table 3: Crystallite size and lattice strain of various samples

<b>Sample</b>	<b>FWHM (2θ°)</b>	<b>Peak position (2θ°)</b>	<b>Crystallite size (Å)</b>	<b>Lattice strain (%)</b>
<b>6500</b>	0.2509	42.4841	530	0.183
<b>6501</b>	0.2244	42.4980	490	0.218
<b>6503</b>	0.2448	42.5855	437	0.269
<b>6505</b>	0.2652	42.5159	396	0.260
<b>8500</b>	0.2244	42.3987	490	0.246
<b>8501</b>	0.2342	42.3827	463	0.257
<b>8503</b>	0.2856	42.4445	361	0.316
<b>8505</b>	0.2856	42.4728	361	0.316

Table 3 showed the crystallite size and lattice strain calculated with FWHM at plane (101) (most significant peak of MgB<sub>2</sub>) at its particular peak positions. The FWHM at (101) increases as the SiC addition increases signified that the degradation of crystallinity. The FWHM increases even larger at higher temperature indicated that the crystallinity degrades even more.

Besides, the peaks are slightly shift to the right with the increasing of addition showing that the original structure of the MgB<sub>2</sub> is distorted due to impurities. The crystallite size and lattice strain are calculated by using the X'Pert Highscore software. It is shown that the crystallite size decreases as the addition level increases while higher temperature gives smaller crystallite size. Samples 8503 and 8505 showed the smallest crystallite size of 361Å while the 6500 gives the largest crystallite of 530Å. In contrast, the lattice strain increases as the temperatures and addition level increase probably because of more impurities are incorporated inside the lattices and induced more micro-strain.

Table 4 shows the lattice parameters analysis of the samples. The lattice parameters and unit cell volume are generated from the Rietveld's Refinement using X'Pert Plus software. The *a*-axis shrinks gradually while the *c*-axis expands slightly as the doping level increases for samples sintered at both temperatures. Higher sintering temperature gives even smaller *a*-axis while the *c*-axis does not vary largely compared to low temperature sintered samples. Shrinking in *a*-axis at high temperature indicated that more impurities or carbon that have been released from the reaction between Mg-SiC have been incorporated easily than in lower sintering temperature while sintering temperature did not affect the *c*-axis much [24]. This shows that the sintering temperature affect more on the *ab*-plane by introducing more impurities than in *c*-plane. This is in relation with the FWHM observed at (101) as the formation of Mg<sub>2</sub>Si and C-incorporation by the reaction of Mg-SiC has a refining effect on the grain growth, thus, the crystallite size has became smaller [22] and the samples tend to be more amorphous at higher sintering temperature. The unit cell volume shrinks from 29.0765Å<sup>3</sup> in 6500 to 29.0067 Å<sup>3</sup> in 6505. Comparing 6505 and 8505, the unit cell volumes are 29.0067Å<sup>3</sup> and 28.9716Å<sup>3</sup> respectively in agreement with the lattice strain calculated as the unit structure is heavily distorted with increasing temperature.  $\Delta(c/a)$  is used as an indicator of the lattice distortion. It indicates that the distortion increases as the addition level increases. At low temperature, the distortion started from 6503 with the value of  $\Delta(c/a) = 0.0014$  while at high temperature the distortion started from 8501 with a comparable value of  $\Delta(c/a) = 0.0013$ . This probably indicates that C substitution at B site is easier to occur at higher temperature than lower temperature. The *x*, as the estimation of C doping level in B is calculated as in [25]:  $x = 7.5 \cdot \Delta(c/a)$ . It shows that the doping level increases with increasing addition and temperature. The estimation further confirmed that C substitution is higher in 8505 than in 6505 with the *x* value of 0.0218 and 0.0138, respectively. This again indicated that high sintering temperature favors C-doping at B sites over lower sintering temperature.

Table 4: Lattice parameters analysis of various samples

Sample	$a$ (Å)	$c$ (Å)	$V$ (Å <sup>3</sup> )	$c/a$	$\Delta(c/a)$	$\text{Mg}(\text{B}_{1-x}\text{C}_x)_2$
6500	3.0863(1)	3.5248(2)	29.0765	1.1421	0.0000	0.0000
6501	3.0854(1)	3.5239(1)	29.0521	1.1421	0.0000	0.0003
6503	3.0835(2)	3.5258(3)	29.0320	1.1434	0.0014	0.0102
6505	3.0822(4)	3.5257(5)	29.0067	1.1439	0.0018	0.0136
8500	3.0860(1)	3.5247(2)	29.0700	1.1422	0.0000	0.0000
8501	3.0832(1)	3.5256(1)	29.0247	1.1435	0.0013	0.0100
8503	3.0810(1)	3.5262(2)	28.9882	1.1445	0.0023	0.0176
8505	3.0799(2)	3.5267(3)	28.9716	1.1451	0.0029	0.0218

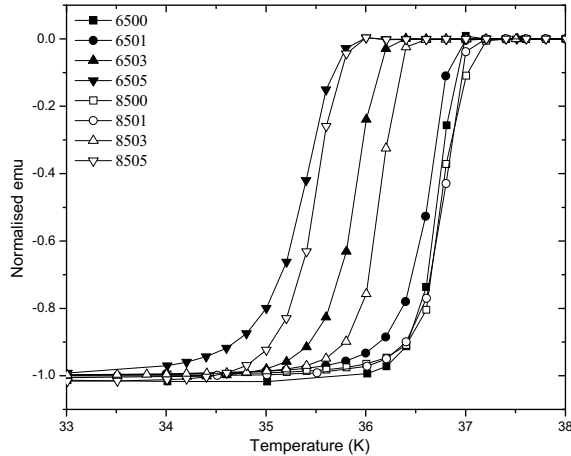


Figure 2: Normalised emu versus temperature for samples sintered at 650°C and 850°C

Figure 2 shows the  $T_c$  of all samples. It is observed that 6500, 8500 and 8501 shares the same  $T_c$  of 36.8K, the highest  $T_c$  achieved among the series. From figure 2, it is noticed that samples sintered at high temperature generally have higher  $T_c$ . This is probably due to the formation of less secondary phases such as  $\text{Mg}_2\text{Si}$  and  $\text{MgO}$  as shown in Table 2, thus, more  $\text{MgB}_2$  is able to be retained to contribute for higher  $T_c$ . With the addition level increases, the  $T_c$  drops gradually for both samples from 36.8K in 6500 and 8500 to 35.1K in 6505 and 35.4K in 8505 respectively. Moreover, the transition width,  $\Delta T$ , increases gradually with the addition level for both sintering temperatures. It increases from 0.2K in 6500 to nearly 1.0K in 6505 while this is 0.2K for 8500 and 0.6K for 8505. From the  $\Delta T$ , it is learnt that lower sintering temperature produces larger transition width, probably resulted from incompleteness of  $\text{MgB}_2$  phase formation and more secondary phases.

#### IV. CONCLUSIONS

The effects of sintering temperature on the phase formation, crystallinity and  $T_c$  of nano-SiC added  $\text{MgB}_2$  were evaluated. With increasing nano-SiC additions, more secondary phases are present, especially  $\text{Mg}_2\text{Si}$  and  $\text{MgO}$ . Also, the samples tend to be more amorphous-like. Phase analysis showed that the crystallite size decreases as the temperature and the addition increases, conversely, lattice strain increases along the addition and temperature. Lattice parameters analysis showed that  $a$ -

axis and unit cell volume decreases gradually as the addition and temperature increases while estimated C-doping increases steadily with increasing addition and temperatures. The  $T_c$  was found to decrease from 36.8K for the 6500 and 8500 to 35.1K in 6505 and 35.4 for 8505. This work shows that appropriate sintering temperature is crucial for enhancing phase formation and  $T_c$  of  $\text{MgB}_2$ .

#### ACKNOWLEDGMENT

The authors would like to acknowledge the financial support from Ministry of Science, Technology and Innovation Malaysia (MOSTI) under the Science Fund 03-01-04-SF0920.

#### REFERENCES

- [1] J. Akimitsu and T. Muranaka, *Physica C* **388-389**, 98 (2003).
- [2] C. Buzea and T. Yamashita, *Superconductor Science and Technology* **14**, R115 (2001).
- [3] H. Kumakura, Y. Takano, H. Fujii, K. Togano, H. Kito, and H. Ihara, *Physica C* **363**, 179 (2001).
- [4] Y. G. Zhao, X. P. Zhang, P. T. Qiao, H. T. Zhang, S. L. Jia, B. S. Cao, M. H. Zhu, Z. H. Han, X. L. Wang, and B. L. Gu, *Physica C* **366**, 1 (2001).
- [5] B. H. Jun, N. K. Kim, K. S. Tan, and C. J. Kim, *Physica C* **469**, 1512 (2009).
- [6] S. M. Hwang, J. H. Choi, E. C. Park, J. H. Lim, J. Joo, W. N. Kang, and C. J. Kim, *Physica C* **469**, 1523 (2009).
- [7] H. Kumakura, A. Matsumoto, H. Fujii, H. Kitaguchi, and K. Togano, *Physica C* **382**, 93 (2002).
- [8] D. H. Kim, J. Chung, T. J. Hwang, W. N. Kang, and K. C. Chung, *Physica C* **469**, 1950 (2009).
- [9] D. Daghero, G. A. Ummarino, M. Tortello, D. Delaude, R. S. Gonnelli, V. A. Stepanov, M. Monni, and A. Palenzona, *Superconductor Science and Technology* **22**, 025012 (2009).
- [10] X. Zhang, Y. Ma, Z. Gao, Z. Yu, G. Nishijima, and K. Watanabe, *Superconductor Science and Technology* **19**, 699 (2006).
- [11] Y. Zhang, S. H. Zhou, C. Lu, K. Konstantinov, and S. X. Dou, *Superconductor Science and Technology* **22**, 015025 (2009).
- [12] E. Bayazit, S. Altin, M. E. Yakinci, M. A. Aksan, and Y. Balci, *J. Alloys Compounds* **457**, 42 (2008).
- [13] R. K. Singh, Y. Shen, R. Gandikota, D. Wright, C. Carvalho, J. M. Rowell, and N. Newman, *Superconductor Science and Technology* **21**, 025012 (2008).
- [14] S. X. Dou, A. V. Pan, S. Zhou, M. Ionescu, H. K. Liu, and P. R. Munroe, *Superconductor Science and Technology* **15**, 1587 (2002).

- [15] Z. Ma, Y. Liu, W. Hu, Z. Gao, L. Yu, and Z. Dong, *Scr. Mater.* **61**, 836 (2009).
- [16] K. Vinod, N. Varghese, S. B. Roy, and U. Syamaprasad, *Superconductor Science and Technology* **22**, 055009 (2009).
- [17] J. H. Lim, S. H. Jang, S. M. Hwang, J. H. Choi, J. Joo, W. N. Kang, and C. J. Kim, *Physica C* **468**, 1829 (2008).
- [18] A. Matsumoto, H. Kitaguchi, and H. Kumakura, *Superconductor Science and Technology* **21**, 065007 (2008).
- [19] A. Gupta and A. V. Narlikar, *Superconductor Science and Technology* **22**, 125029 (2009).
- [20] C. M. Lee, J. H. Park, S. M. Hwang, J. H. Lim, J. Joo, W. N. Kang, and C. J. Kim, *Physica C* **469**, 1527 (2009).
- [21] M. Mudgel, V. P. S. Awana, H. Kishan, and G. L. Bhalla, *Solid State Commun.* **146**, 330 (2008).
- [22] B. Qu, X. D. Sun, J. G. Li, Z. M. Xiu, and C. P. Xue, *Superconductor Science and Technology* **22**, 075014 (2009).
- [23] J. H. Kim, S. X. Dou, D. Q. Shi, M. Rindfleisch, and M. Tomsic, *Superconductor Science and Technology* **20**, 1026 (2007).
- [24] J. H. Lim, J. H. Shim, J. H. Choi, J. H. Park, W. N. Kim, J. Joo, and C. J. Kim, *Physica C* **469**, 1182 (2009).
- [25] M. Avdeev, J. D. Jorgensen, R. A. Ribeiro, S. L. Bud'ko, and P. C. Canfield, *Physica C* **387**, 301 (2003).

## Authors' informations

*Mr. Tan Kwee Yong\** is with the Dept. of Physics, Faculty of Science, Universiti Putra Malaysia, 43400 UPM Serdang, Malaysia (\*corresponding author's phone: +6016-7688345; fax: +603-8946 4454; e-mail: kweeyong@gmail.com).

Ms. Tan Kim Lee is with the Dept. of Physics, Faculty of Science, Universiti Putra Malaysia, 43400 UPM Serdang, Malaysia (author's phone: +6012-6378151; fax: +603-8946 4454; e-mail: faviscamp@hotmail.com).

Prof. Dr. Abdul Halim Shaari is with the Dept. of Physics, Faculty of Science, Universiti Putra Malaysia, 43400 UPM Serdang, Malaysia (author's phone: +603-8946 6648; fax: +603-8946 4454; e-mail: ahalim@science.upm.edu.my).

Dr. Chen Soo Kien is with the Dept. of Physics, Faculty of Science, Universiti Putra Malaysia, 43400 UPM Serdang, Malaysia (author's phone: +603-8946 6668; fax: +603-8946 4454; e-mail: skchen@science.upm.edu.my).

Dr. Tan Kar Ban is with the Dept. of Chemistry, Faculty of Science, Universiti Putra Malaysia, 43400 UPM Serdang, Malaysia (author's phone: +603-8946 6776; fax: +603-8946 5380; e-mail: tankb@science.upm.edu.my).